EPSC Abstracts,
Vol. 4, EPSC2009-734, 2009
European Planetary Science Congress,

The effect of solar wind conditions upon the atmospheric boundary layers at Venus.

I. Whittaker (1), M. Grande (1), G. Guymer (1), S. Barabash (2), T. Zhang (3) and the ASPERA team.

(1) Aberystwyth University, UK. (2) Swedish Institute of Space Physics, Kiruna, Sweden. (3) Space Research Institute, Austrian Academy of Sciences, Graz, Austria. (icw06@aber.ac.uk)

Introduction

Venus has been of interest to researchers for many years due to its similarity and proximity to Earth. The planet has no measurable dipole magnetic field and hence the solar wind can interact directly with the ionosphere and erode the cold planetary plasma. Venus Express (VEX) is currently orbiting the planet in a highly elliptical polar orbit, with periapsis around 180 km and an orbital period of 24 hours.

The ASPERA-4 instrument mounted on VEX is an atmospheric analysis package comprising electron spectrometer, neutral particle detector, neutral particle imager and a separately mounted ion mass spectrometer [1]. The data for this investigation is taken from the IMA (ion mass analyser) part of the ASPERA package, along with additional data taken from the MAG (Magnetometer) instrument [2] also mounted on VEX. All positional data is given in Venus-centric orbital coordinates. In this system the x axis is the Venus – Sun line, the y axis is the tangent to the orbital motion and the z axis points up the rotational axis.

The solar wind interaction has been studied extensively at Venus with the Pioneer Venus Orbiter mission. The solar wind is slowed by the interaction with the planetary bow shock. Since Venus is non-magnetic, the IMF drapes horizontally over the atmosphere. Inside the bow shock the compressed field lines form a pressure balance with the ionosphere resulting in an inner boundary layer [3]. Workers with magnetic data commonly refer to this boundary as the magnetic pile-up boundary. However, as this study is using ion data we will refer to the ion composition boundary (ICB).

Boundary fitting

Figure 1a shows a typical energy time plot showing total ion counts in a dayside to night side pass, as seen by IMA, with the main features indicated.

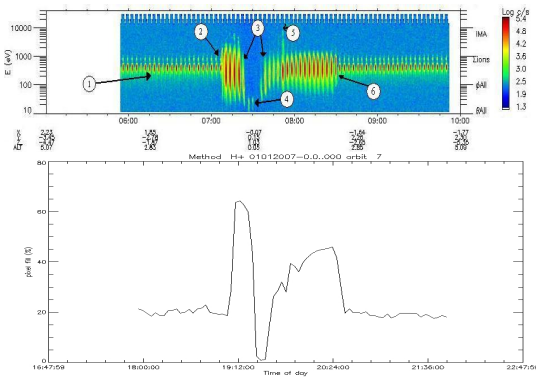

Figure 1: (a) An ion orbit plot for 18th Jan 2007. (b) A pixel fill plot for the same date.

Point (1) shows the incident upstream solar wind. The superalfvenic wind then creates the planetary bow shock at (2), as the solar wind ions drop to a subsonic speed with a much greater (shocked) energy spread. The magnetosheath region meets the ICB at (3). Within this (4), lies a region of cold ionospheric planetary plasma, shielded by the ICB. The ICB (3) is then crossed again and the wake region is characterised by a slow increase of solar wind penetration until (5) where the data regains the appearance of shocked solar wind. Also this point (5) shows a single spectrum with greater energy spread, indicative of atmospheric escape. Point (6) shows VEX returning to the solar wind. Since IMA scans all energies along a single elevation range before moving to the next elevation, the spectra appear as a series of discrete scans.

A bow shock model has been produced from four months of data comprising October 2006 to January 2007; this was then fitted using an occupational probability weighting function, derived by determining the VEX speed at that. The data was then checked with a 14 month ion map as shown in Figure 2. The left plot is an *x-y* plot, the right picture is a cylindrical plot with

EPSC Abstracts,
Vol. 4, EPSC2009-734, 2009
European Planetary Science Congress,

the *r* values signed with the *y* value. The bow shock model has been overplotted for both, indicating that the fitting method works well.

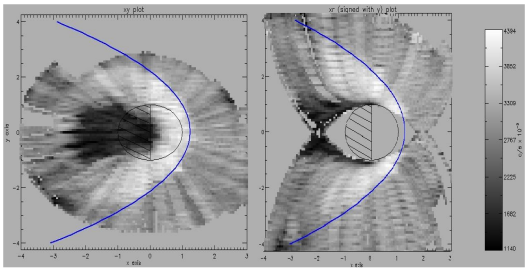

Figure 2: Ion maps with the current bow shock model.

The boundary positions from Figure 1a are easy to recognise. However, for reproducibility, a boundary recognitoin algorithm is used. Each spectrum scan is analysed individually and characterised by how many pixels are above a noise value.

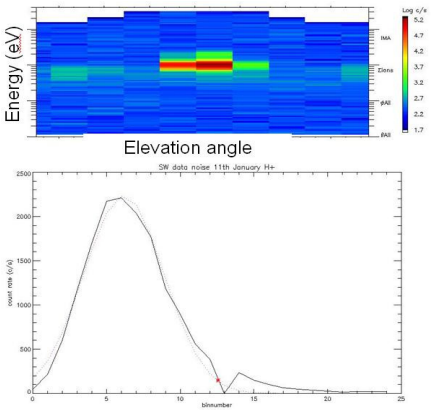

Figure 3: A binned plot to determine the noise value.

Figure 3 shows an example. Data is binned and a Gaussian fitted; the maximum noise count cut-off is set at twice the standard deviation from the peak, as marked by the red star. All spectra throughout the orbit are then analysed and a percentage of pixels above this threshold is plotted against time. Figure 1b gives an example of this, a boundary crossing is then determined to occur when any two points differ in signal by 20% or more.

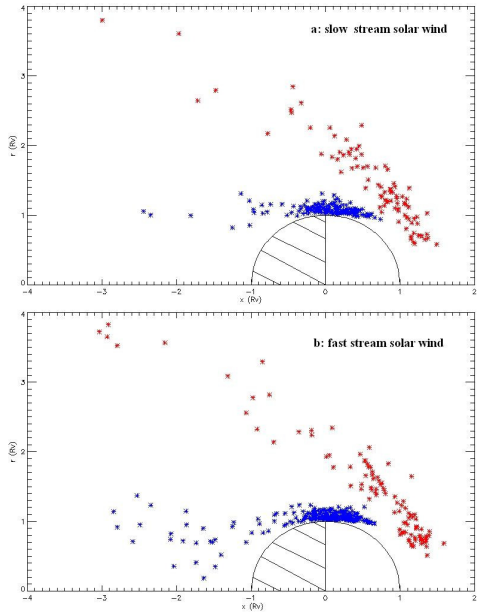

Figure 4: Algorithm derived bow shock (red) and ICB (blue) crossings.

Comparing the conditions to the data

The crossing points derived from the algorithm covering 14 months of 2007 and 2008 can be seen in Figure 5; they split naturally into bow shock (red) and ICB crossings (blue). The ICB has previously been fitted, and compared to solar wind conditions [4], however it was not characterised, as here, solely from ion data.

The results shown in Figure 4 are split by mean solar wind speed. The upper plot (4a) is for solar wind below 850 eV and the lower plot (4b) is for solar wind above this value. The higher energy solar wind spreads out over a greater area into the tail and hence produces a more varied ICB response. The algorithm also seems to be better at detecting boundaries at faster solar wind speeds.

References

[1] Barabash S. et al. (2007). *PSS 55(12) 1772-1792*

[2] *Zhang T. L. et al.* (2006). *PSS 54 1336-1343*

[3] Russell C. T. and Vaisberg O. (1983). *Venus, University of Arizona Press*. 873-940

[4] Martinecz C. et al. (2008). *JGR 114 doi:10.1029/2008JE003174.*